Journal of Molecular Liquids 264 (2018) 48–53

Contents lists available at ScienceDirect

Journal of Molecular Liquids

journal homepage: www.elsevier.com/locate/molliq

Zwitterions of the excited 4-([2,2′-bipyridine]-4-yl) phenol photoacid molecules: Formation and fluorescence

Guanghua Ren [a,c,1], Qingchi Meng [a,c,1], Jinfeng Zhao [a], Tianshu Chu [a,b,*]

[a] State Key Laboratory of Molecular Reaction Dynamics, Dalian Institute of Chemical Physics, Chinese Academy of Sciences, Dalian 116023, PR China
[b] Institute for Computational Sciences and Engineering, Laboratory of New Fiber Material and Modern Textile, the Growing Base for State Key Laboratory, Qingdao University, Qingdao 266071, PR China
[c] University of the Chinese Academy of Sciences, Beijing 100049, PR China

ARTICLE INFO

Article history:
Received 9 March 2018
Received in revised form 26 April 2018
Accepted 12 May 2018
Available online 12 May 2018

Keywords:
Photoacid molecules
Zwitterion
Proton-coupled electron transfer
Fluorescence emission
TDDFT

ABSTRACT

Based on the density functional theory and time-dependent density functional theory, we have investigated the zwitterionic structure of the excited 4-([2,2′-bipyridine]-4-yl) phenol (bpy-phenol) photoacid molecules. The zwitterion can be formed stepwisely via a proton-coupled electron transfer (PCET) reaction in a H-bonded bpy-phenol…F^- complex and an intermolecular excited state proton transfer (ESPT) reaction between HF molecules and excited deprotonated anions of bpy-phenol. Supported by the results of Hirshfeld population analysis and electrostatic potential, a basic site was generated in the bpy residue due to the PCET process. With a proper F^- ions concentration, the ESPT reaction can be occurred with little barrier between the HF molecules and the bpy-phenol anions, leading to the generation of zwitterions. Moreover, the zwitterion fluoresces at 550 nm, which is longer than that of bpy-phenol anions at 490 nm. Our finding not only discovers the zwitterionic process of photoacid molecules, but also pioneers a frontier field of activity study after PCET reactions.

1. Introduction

Proton-coupled electron transfer (PCET) reactions exist widely in activities of biology and chemistry, such as photosynthesis, respiration and solar fuel cells [1–4]. According to previous studies, the mechanism of PCET could be as that protons and electrons transfer concertedly or stepwisely [5]. PCET reactions are sensitive to electronic structures of molecules and usually have close relations with H-bonds [6–8]. In general, the overall strength of H-bonds will be enhanced or weakened after optical excitation, resulting in photophysical and photochemical changes, such as intramolecular charge transfer (ICT), photo-induced electron transfer (PET), fluorescence resonance energy transfer (FRET), excited state proton transfer (ESTP), etc. [9–15] H-bonds often provide pre-set pathways for intermolecular ESPT, a common phenomenon in photoacid-base H-bonding complexes [11,13,16]. Photoacids own greater ability to provide protons after absorbing photons. However, some photoacids not only have acidic sites to be deprotonated but also have basic sites to be protonated [17–18]. Within such kind of photoacids, besides intermolecular ESPT, ICT can also occur. As such, PCET in a photoacid-base complex is featured by an intermolecular ESPT following an ICT within hundreds of femtoseconds, which makes the complex stay in a state of charge separation [19]. The nature of this charge separation is the spirit of photosynthesis. However, few studies focus on the events after the PCET charge separation process, although they are important in the biological and material fields.

Charge-separation configurations after PCET, known as zwitterions, are ubiquitous in chemical and biological processes [20–22]. Some amino acids and neurotransmitters have no net charge at physiological conditions, but they exist as zwitterions with the carboxyl deprotonated and one of the nitrogen atoms protonated [23]. Due to favorable noncovalent interactions, the zwitterionic structures are also crucial for self-assembly and design of conductive materials [24]. The prototypes of these zwitterions share one common feature that the acidic site and the basic site are located in the same molecule but at opposite positions. However, the zwitterionic forms of photoacids with both acidic sites and basic sites have received relatively little attention. It is therefore interesting and necessary to extend the studies on the capabilities and characteristics of the photoacids in their zwitterionic forms, except the common features such as proton pumps and fluorescent indicators.

Recently, a new synthetic photoacid, 4-([2,2′-bipyridine]-4-yl) phenol, has been reported by Sandeep Verma et al. [18] This photoacid is a typical phenol derivative with both acidic and basic sites, and can also be viewed as an analogue of tyrosine. For simplicity, we termed it as

* Corresponding author at: State Key Laboratory of Molecular Reaction Dynamics, Dalian Institute of Chemical Physics, Chinese Academy of Sciences, Dalian 116023, PR China.
E-mail address: tschu@dicp.ac.cn (T. Chu).
[1] These authors contribute equally to this work.

https://doi.org/10.1016/j.molliq.2018.05.052
0167-7322/

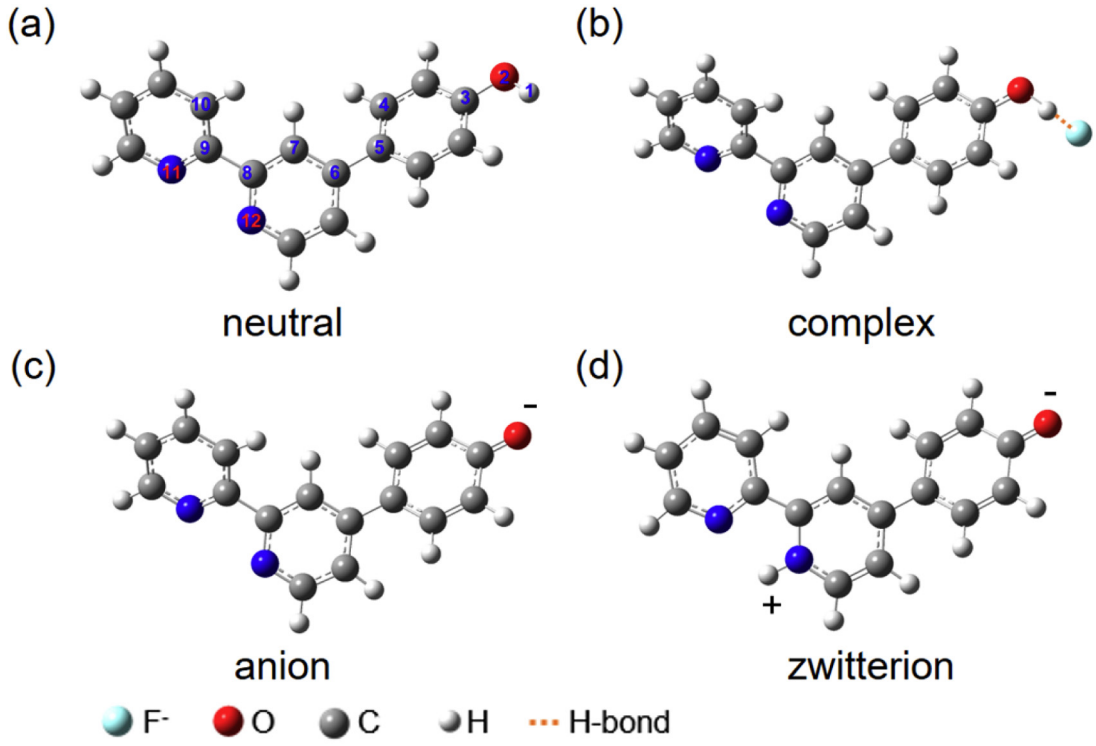

Fig. 1. Schematic illustration of bpy-phenol in the form of (a) neutral, (b) complex, (c) anion and (d) zwitterion.

bpy-phenol below. It can be used as anion probes, especially for F^- anions. In the above-mentioned work, photoexcitation of the bpy-phenol molecule led to a PCET reaction including an ICT from phenol to the bpy residue and a proton transfer from the phenol to the F^- ion. The timescales of ESPT was 150 femtoseconds, indicating a strong H-bonding effect between the phenol hydroxyl and the base F^- ion [25]. However, the fluorescent phenomena in this experiment were unique. The three emission bands peaking at 400, 490 and 550 nm were assigned to the neutral, deprotonated anionic and H-bonding complex form of bpy-phenol, respectively. According to the H-bonding effects on spectra, it is uncommon for the H-bonding complex to emit a lower energy photon than the anionic one [8,14,26–27]. Such a rare experimental result means that there is lying something undetected for the bpy-phenol molecule after the PCET reaction, which deserves further investigation.

In this work, density functional theory (DFT), time-dependent DFT [28] (TDDFT) and wave function analysis [29] (WFA) methods have been used to explore the unclear fluorescent mechanism of the newly synthesized bpy-phenol molecule. Results from Hirshfeld population analysis [30] (HPA), the calculated electrostatic potential [31] (ESP), potential energy surfaces (PESs) and absorption and emission spectra, all evidenced and supported that a bpy-phenol zwitterion has been generated after the PCET reaction, which, instead of the H-bonding complex, is responsible for the emission band centering around 550 nm.

2. Computational details

All theoretical calculations were performed by dispersion-corrected [32] DFT and TDDFT methods and carried out in Gaussian 16 program suite [33]. The HPA and ESP results were obtained via Multiwfn suite [34]. All the molecular geometries in the ground S_0 state and the excited S_1 state were fully optimized without any constraints at the level of M06-2X [35] /6-311 + G** [36] and TD-M06-2X/6-311 + G**, respectively. Vibrational frequency calculations have been used to analyze the optimized structures to conform that these structures corresponded to the local minima with no imaginary frequency. The excited-state PESs along two proton transfer coordinates were obtained at TD-M06-2X/TZVP [37] level. The absorption and emission spectra were calculated by TD-PBE0 [38] method with TZVP basis set. In all the calculations, the acetonitrile solvent was selected and performed with the continuum solvation model based on solute electron density (SMD) method [39].

Table 1
Primary bond length (Å), dihedral angle (°) and relative energy (kcal/mol) of the neutral and zwitterion of bpy-phenol in the S_0 and S_1 states. δ: dihedral angle. E: the amount of energy relative to the S_0 state of the neutral form, only including the neutral and zwitterion of bpy-phenol due to the same numbers of atoms. Atom labels are marked in Fig. 1.

Electronic state	Neutral		Complex		Anion		Zwitterion	
	S_0	S_1	S_0	S_1	S_0	S_1	S_0	S_1
H-bond	–	–	1.252	1.016	–	–	–	–
H_1-O_2	0.966	0.971	1.097	1.365	–	–	–	–
O_2-C_3	1.358	1.332	1.321	1.274	1.266	1.245	1.252	1.243
C_5-C_6	1.482	1.403	1.478	1.421	1.468	1.439	1.454	1.436
C_8-C_9	1.494	1.492	1.494	1.486	1.495	1.467	1.485	1.452
δ(C_4-C_5-C_6-C_7)	−33.1	−0.5	−30.9	−0.5	−26.1	−13.8	−28.7	−14.4
δ(C_7-C_8-C_9-C_{10})	−34.1	−33.4	−35.2	−26.4	−35.1	−14.7	9.6	0.0
E	0.0	93.7	–	–	–	–	8.8	69.5

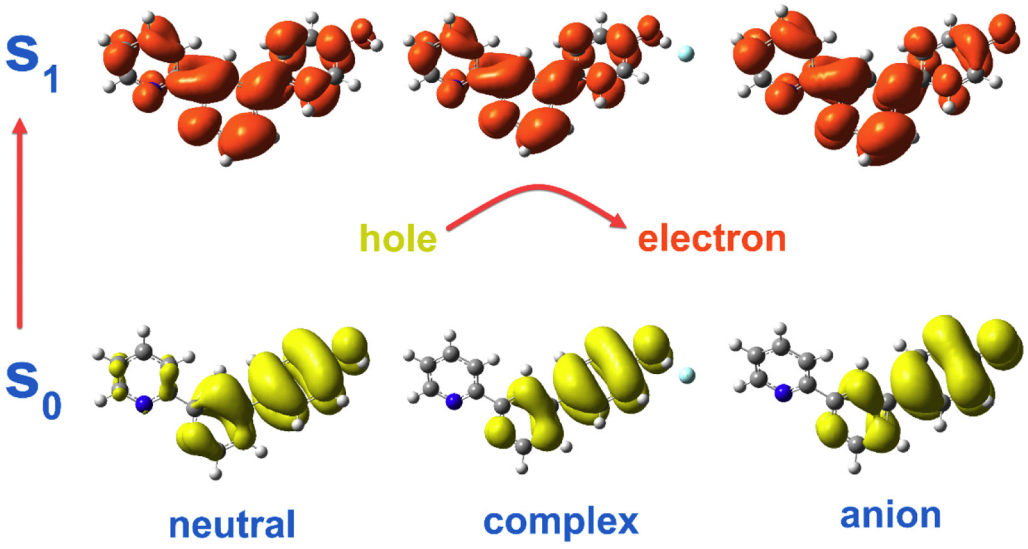

Fig. 2. Hole-electron transition for neutral, complex and anionic bpy-phenol. Electrons are excited from hole to electron. Yellow: holes. Red: electrons.

3. Results and discussion

3.1. Geometric structures in the S_0 and S_1 states

The optimized structures in S_0 state of neutral, H-bonding complex, anionic and zwitterion of bpy-phenol are presented in Fig. 1. The corresponding changes in structural parameters from S_0 to S_1 state are summarized in Table 1. As seen, the bond H_1-O_2 in S_1 state is lengthened; especially for the complex, with an increment of 0.268 Å when compared with that in S_0 state. Meanwhile, in the S_1 state, the length of O_2-C_3, C_5-C_6 and C_8-C_9 are all shortened and the dihedral angles δ(C_4-C_5-C_6-C_7) and δ(C_7-C_8-C_9-C_{10}) become smaller. This clearly shows that, the geometrical configurations become more compact and coplanar upon photoexcitation. Besides, being shortened by 0.236 Å, the intermolecular H-bond in the complex becomes strengthened after the molecule is pumped to the excited state. Comparing to the relative energy between the neutral and zwitterion, the S_1 state of zwitterion is more stable than the S_1 state of neutral form. This indicates that the excited neutral bpy-phenol can be a precursor for the zwitterion, which will be described below.

3.2. Hirshfeld charge population in S_0 and S_1 states

An acidic site and a basic site are prerequisites for generating the zwitterion [40]. In bpy-phenol, the acidic site is the phenol hydroxyl, which is definite due to the unique structures of photoacids. To figure out the basic site, the charge distribution in the S_0 and S_1 states was studied qualitatively and quantitatively through electronic transition and HPA, respectively. Fig. 2 shows the electronic transition from S_0 to S_1 state, where the yellow area, named hole, represents the distribution of electrons that to be excited, and the red region called electron stands for the distribution of electrons that have been excited. As we can see, there exists electron transfer from phenol residue to bi-pyridine residue. Very likely, the basic site should exist in the bi-pyridine residue. For further confirmation, the HPA was applied to quantitatively describe the variation of charge population and the corresponding results are presented in Table 2. To facilitate the statements, we take Q (1–2) as the sum quantity of the charges on atom H_1 and O_2. Similar conventions are applied for Q (3–5), Q (6–10) and Q (11–12). There are at least four features that can be seen from Table 2. First, after photo-absorption, Q (1–2) and Q (3–5) are getting more positive while Q (6–10) and Q (11–12) are getting more negative, suggesting that charges transfer from phenol residue to bi-pyridine residue. Second, Q (11–12) is the most negative, indicating a potential basic site could be existed near the two N atoms. Third, from the neutral form to the anionic form in S_1 state, with the proton gradually transferring away from phenol residue, the Q (11–12) also gets more and more negative, reflecting the inherent nature of PCET mechanism. Fourth, after excitation, the molecular dipole moment of the neutral bpy-phenol gets larger, whereas the corresponding values in complex and anionic forms become smaller. This difference originates from the different charge populations. Compared with the neutral bpy-phenol, the deprotonated anion and H-bonding complex both have one net negative charge. And the net negative charge mainly distributes near the O_2 atom and the F^- ion in S_0 states, but transferred to their bpy residues in S_1 states. This kind of CT caused by optical excitation makes the dipole moments of the deprotonated anion and the H-bonding complex become smaller. However, with no net charge in the neutral bpy-phenol, the phenol hydroxyl becomes more positive and the two N atoms become more negative after being excited, making the dipole moment of the neutral one turn larger. The charge transfer characteristics are in accordance with the geometrical changes shown in the above section. That is to say, the electron density decreases when the bond lengths become longer while it increases when the bond lengths and dihedral angles become shorter and smaller. In order to exactly determine the position of the basic site, in the following section, the ESP method is used to quantitatively measure the molecule's capability of being protonated.

3.3. Electrostatic potential on the van der Waals surface

To further confirm the basic site, we calculate the ESP on the Van der Waals surface in the S_0 and S_1 states. ESP is of vital importance to

Table 2
Hirshfeld charge distribution on primary atoms and the molecular dipole moment in S_0 and S_1 states for neutral, complex and anionic bpy-phenol. Q: quantity of electric charge. D: dipole moment.

State	Neutral		Complex		Anion	
	S_0	S_1	S_0	S_1	S_0	S_1
Q (F^-)	–	–	−0.572	−0.389	–	–
Q (1–2)	−0.01	0.068	−0.232	−0.180	−0.501	−0.372
Q (3–5)	0.007	0.113	−0.038	0.059	−0.124	0.043
Q (6–10)	0.001	−0.089	−0.009	−0.143	−0.033	−0.181
Q (11–12)	−0.399	−0.455	−0.406	−0.492	−0.419	−0.512
D	1.497	4.380	9.829	4.485	7.140	1.602

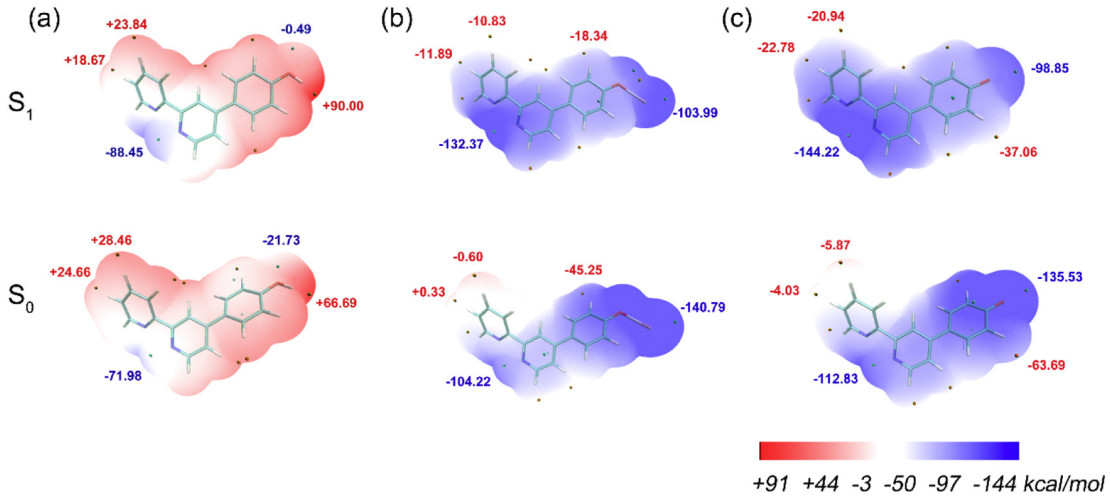

Fig. 3. Electrostatic potential (ESP) on the Van der Waals surface. Rows from top to bottom are S_1 and S_0 states. Columns from left to right are neutral, complex and anionic bpy-phenol. Maximum points are marked by red and minimum points are marked by blue.

determine the reactivity between two molecules [41]. In Fig. 3, some extreme points of ESP on the surface are marked with their corresponding values at the fully optimized S_0 and S_1 geometries. It shows that, after optical excitation, the ESP becomes more positive in the phenol part and more negative in the bi-pyridine part, which is consistent with the Hirshfeld charge distribution. In every form of bpy-phenol, the global minimum of ESP is near the N_{12} atom in S_1 state. Besides, among these global minimum points in all the forms of bpy-phenol, the site near N_{12} atom of the anionic bpy-phenol in S_1 state gets the most negative ESP value with a scale of −144.22 kcal/mol. This fact indicates that after the PCET process in the complex, the most basic site has transformed from the F^- ion to the N_{12} atom. And the zwitterion can be generated if the basic site at N_{12} atom could be protonated.

3.4. Potential energy surface for the proton transfer

According to the absorption spectra and the PCET results in the experimental work [18], there existed HF molecules in solution. In order to verify that the zwitterion of bpy-phenol can be generated with the assistance of HF molecules, we have calculated and constructed the PES on proton transfer along two reaction coordinates: one is the O_2-H_1 coordinate and the other is the N_3-H_4 coordinate. The geometry for this PES is shown in the inset of Fig. 4. As indicated by Fig. 4, the proton transferred along the O_2-H_1 coordinate from phenol hydroxyl to the F^- anion freely, which is in agreement with the ultrafast PCET process. Then, via N_3-H_4 coordinate, it is overwhelming for the proton transfer from the HF molecule to the N_{12} atom. This result approves that after the first proton transfer, the PCET reaction, the charge accumulated N_{12} atom in the anionic bpy-phenol has enough power to attract the proton from HF molecule to generate the more stable zwitterion of bpy-phenol. Therefore, the two stepwise ESPT processes reflected by the PES indicate that the deprotonated anion is a precursor for generating the zwitterion of bpy-phenol, which is further proved by the results from the same calculations on the methylated bpy-phenol (in Fig. S1). In addition, solvent influences on the zwitterions is investigated, and the corresponding results are shown in Fig. S2, demonstrating that solvents with large values

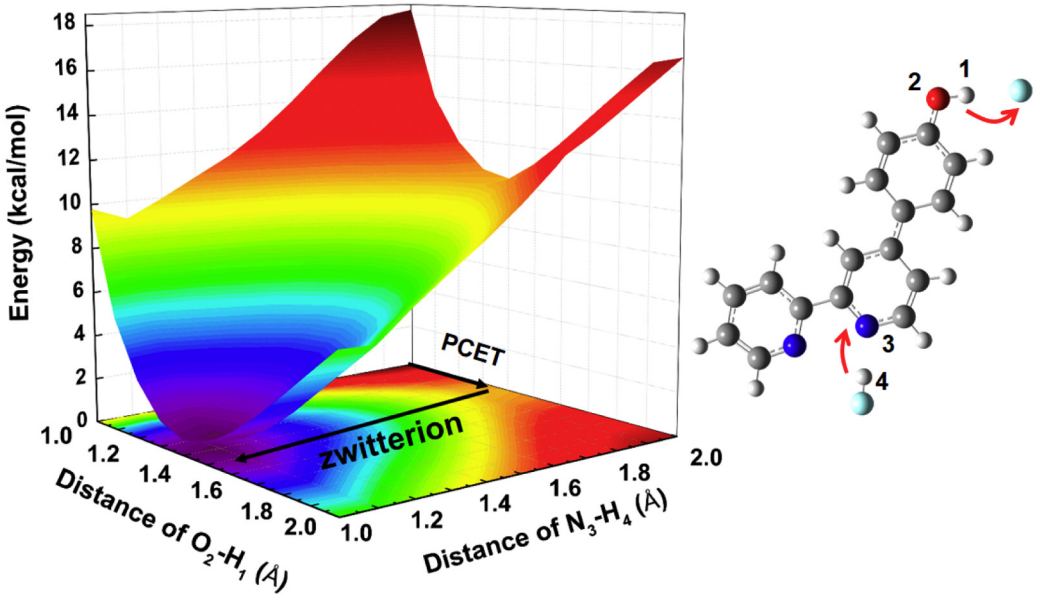

Fig. 4. Potential energy surface (PES) for the zwitterion reaction. Inset is the geometry for the protons transfer along the O_2-H_1 and N_3-H_4 coordinates.

Table 3
The detailed theoretical and experimental spectra data for the forms of neutral, complex, anion and zwitterion of bpy-phenol.

	Electronic transition	Wavelength (nm)	f[a]	Contrib[b]	CI[c]	Exp[d] (nm)
Neutral						
Absorption	$S_0 \rightarrow S_1$	294	0.5818	H → L	0.94	282
Emission	$S_1 \rightarrow S_0$	375	0.9837	L → H	0.98	400
Complex						
Absorption	$S_0 \rightarrow S_1$	332	0.4843	H → L	0.97	330
Emission	$S_1 \rightarrow S_0$	413	0.7128	L → H	0.98	–
Anion						
Absorption	$S_0 \rightarrow S_1$	397	0.3871	H → L	0.98	390
Emission	$S_1 \rightarrow S_0$	491	0.3725	L → H	0.99	490
Zwitterion						
Absorption	–	–	–	–	–	–
Emission	$S_1 \rightarrow S_0$	557	0.6917	L → H	0.99	550

[a] Oscillator strength.
[b] H, highest occupied molecular orbital (HOMO) and L, lowest unoccupied molecular orbital (LUMO).
[c] The CI coefficients in absolute values.
[d] The experimental spectra data from Ref. 18.

of dielectric constant favor the generation of the zwitterionic bpy-phenol.

3.5. Absorption and fluorescence spectra

In order to choose one appropriate method to calculate the spectra of bpy-phenol, some different functionals, including PBE0, M06-2X, B3LYP [42], CAM-B3LYP [43], ωB97XD [44] and LC-ωPBE [45], have been tested with the same TZVP basis set [46–47]. These results are presented in Table S1 in Supporting information. Among these functionals, the PBE0 results fit well with the experimental results. Table 3 lists the detailed spectral data of all the various forms of bpy-phenol that obtained by TD-PBE0/TZVP method and by the experiments. The neutral molecule absorbed at ~294 nm and emitted at ~375 nm. And both absorption and fluorescence bands of the anion display a red shift relative to the neutral ones, for the proton has transferred to the F^- ion. The absorption and emission peaks of the H-bonded bpy-phenol are located at 332 nm and 413 nm, lying between those of neutral molecules and anions, in agreement with the facts that the proton has partially transferred to the F^- ion in the H-bonded complex. Notably, the calculated fluorescence spectra of zwitterions peaked at 557 nm, which is consistent with the experimental results (~550 nm). The lifetimes of the four molecules have also been calculated and compared with the experimental lifetime values in Table S2, showing a reasonable accordance. In addition, the deviations between calculations and experiments in spectra and lifetimes could be resulted from systematic errors including the incompleteness of calculation methods and solvation model. Based on these consequences, the H-bonding complex is likely to lead a PCET reaction rather than emit a photon. This may explain why there was no trace of the fluorescence band of the complex in experiments. Fig. 5 shows the simulated absorption and emission spectra with the PBE0 functional. One thing worth mention here is that we find the generation of zwitterions is favored in solution with a proper F^- concentration. With excess F^- ions, F^-HF^- complex can be formed, whose capability of attracting protons is larger than that of N_{12}. Thus, it becomes harder for N_{12} atom to be protonated and formation of zwitterions will be inhibited under the condition of excess F- ions. The experimental results agree with our predictions [18].

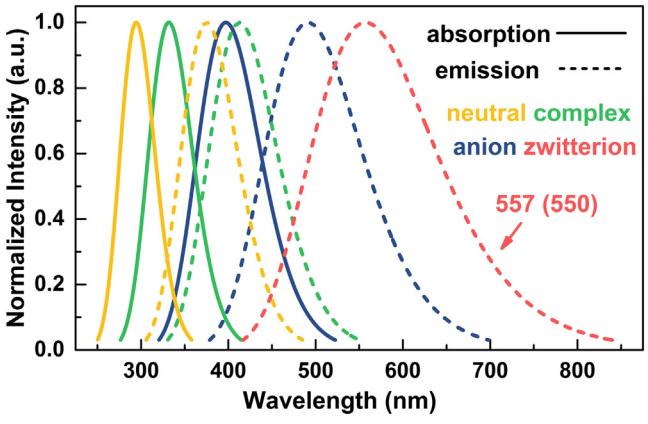

Fig. 5. Simulated absorption and emission spectra with time-dependent PBE0 method. The absorption bands were described with solid line and the emission bands were shown with short dash line. The neutral, H-bonding complex and anionic form of bpy-phenol were colored by yellow, green and blue, respectively. The emission band of zwitterion colored by red was marked with the simulated value and the corresponding experimental result was listed in parentheses. All the geometries mentioned above have been presented in Fig. 1.

4. Conclusions

By applying DFT and TDDFT methods to study the new synthetic photoacid molecule bpy-phenol, we found that, induced by the PCET reaction between the bpy-phenol and F^- ion, a basic site was created near the N atom in the bpy residue. The basic site can be further protonated via accepting proton from the HF molecule to finally generate the zwitterion of bpy-phenol. This zwitterion has a fluorescence band peaking at a wavelength of 550 nm longer than that of the neutral, anion, and H-bonding form. This finding might open a new perspective in the design of zwitterionic materials through photoacids and PCET reactions.

Acknowledgments

This work is supported by the National Natural Science Foundation of China (Grant No. 11604333), the Science Challenging Program (JCKY2016212A501), and the Open Fund of the State Key Laboratory of Molecular Reaction Dynamics in DICP, CAS (SKLMRD-K20180).

Appendix A. Supplementary data

Supplementary data to this article can be found online at https://doi.org/10.1016/j.molliq.2018.05.052.

References

[1] M.H.V. Huynh, T.J. Meyer, Proton-coupled electron transfer, Chem. Rev. 107 (2007) 5004–5064.
[2] T.J. Meyer, M.H.V. Huynh, H.H. Thorp, The possible role of proton-coupled electron transfer (PCET) in water oxidation by photosystem II, Angew. Chem. Int. Ed. 46 (2007) 5284–5304.
[3] A. Migliore, N.F. Polizzi, M.J. Therien, D.N. Beratan, Biochemistry and theory of proton-coupled electron transfer, Chem. Rev. 114 (2014) 3381–3465.
[4] D.R. Weinberg, C.J. Gagliardi, J.F. Hull, C.F. Murphy, C.A. Kent, B.C. Westlake, A. Paul, D.H. Ess, D.G. McCafferty, T.J. Meyer, Proton-coupled electron transfer, Chem. Rev. 112 (2012) 4016–4093.
[5] S. Hammes-Schiffer, A.A. Stuchebrukhov, Theory of coupled electron and proton transfer reactions, Chem. Rev. 110 (2010) 6939–6960.
[6] T.F. Markle, J.M. Mayer, Concerted proton–electron transfer in pyridylphenols: the importance of the hydrogen hond, Angew. Chem. Int. Ed. 47 (2008) 738–740.
[7] M. Sjödin, T. Irebo, J.E. Utas, J. Lind, G. Merényi, B. Åkermark, L. Hammarström, Kinetic effects of hydrogen bonds on proton-coupled electron transfer from phenols, J. Am. Chem. Soc. 128 (2006) 13076–13083.
[8] G.J. Zhao, K.L. Han, Hydrogen bonding in the electronic excited state, Acc. Chem. Res. 45 (2011) 404–413.
[9] G.J. Zhao, J.Y. Liu, L.C. Zhou, K.L. Han, Site-selective photoinduced electron transfer from alcoholic solvents to the chromophore facilitated by hydrogen bonding: a new fluorescence quenching mechanism, J. Phys. Chem. B 111 (2007) 8940–8945.
[10] G.J. Zhao, K.L. Han, Site-specific solvation of the photoexcited protochlorophyllide a in methanol: formation of the hydrogen-bonded intermediate state induced by hydrogen-bond strengthening, Biophys. J. 94 (2008) 38–46.

[11] G.Y. Li, G.J. Zhao, Y.H. Liu, K.L. Han, G.Z. He, TD-DFT study on the sensing mechanism of a fluorescent chemosensor for fluoride: excited-state proton transfer, J. Comput. Chem. 31 (2010) 1759–1765.
[12] J.S. Chen, G.J. Zhao, T.R. Cook, K.L. Han, P.J. Stang, Photophysical properties of self-assembled multinuclear platinum metallacycles with different conformational geometries, J. Am. Chem. Soc. 135 (2013) 6694–6702.
[13] J.S. Chen, P.W. Zhou, S.Q. Yang, A.P. Fu, T.S. Chu, Sensing mechanism for a fluoride chemosensor: invalidity of excited-state proton transfer mechanism, Phys. Chem. Chem. Phys. 15 (2013) 16183–16189.
[14] F. Yu, P. Li, B. Wang, K. Han, Reversible near-infrared fluorescent probe introducing tellurium to mimetic glutathione peroxidase for monitoring the redox cycles between peroxynitrite and glutathione in vivo, J. Am. Chem. Soc. 135 (2013) 7674–7680.
[15] T.S. Chu, B.T. Liu, Establishing new mechanisms with triplet and singlet excited-state hydrogen bonding roles in photoinduced liquid dynamics, Int. Rev. Phys. Chem. 35 (2016) 187–208.
[16] S. Chai, G.J. Zhao, P. Song, S.Q. Yang, J.Y. Liu, K.L. Han, Reconsideration of the excited-state double proton transfer (ESDPT) in 2-aminopyridine/acid systems: role of the intermolecular hydrogen bonding in excited states, Phys. Chem. Chem. Phys. 11 (2009) 4385–4390.
[17] J. Sérgio Seixas de Melo, A.N.L. Maçanita, Unveiling the Eigen-Weller ion pair from the excited state proton transfer kinetics of 3-chloro-4-methyl-7-hydroxycoumarin, J. Phys. Chem. B 119 (2014) 2604–2610.
[18] S. Verma, S. Aute, A. Das, H.N. Ghosh, Proton-coupled electron transfer in a hydrogen-bonded charge-transfer complex, J. Phys. Chem. B 120 (2016) 10780–10785.
[19] M. Kuss-Petermann, O.S. Wenger, Photoacid behavior versus proton-coupled electron transfer in phenol–Ru (bpy) 32+ dyads, J. Phys. Chem. A 117 (2013) 5726–5733.
[20] J.G. Kirkwood, Theory of solutions of molecules containing widely separated charges with special application to zwitterions, J. Chem. Phys. 2 (1934) 351–361.
[21] O. Perraud, V. Robert, H. Gornitzka, A. Martinez, J.P. Dutasta, Combined cation–π and anion–π interactions for zwitterion recognition, Angew. Chem. Int. Ed. 51 (2012) 504–508.
[22] T. Rodgers, M. Rowland, Physiologically based pharmacokinetic modelling 2: predicting the tissue distribution of acids, very weak bases, neutrals and zwitterions, J. Pharm. Sci. 95 (2006) 1238–1257.
[23] M. Gutowski, P. Skurski, J. Simons, Dipole-bound anions of glycine based on the zwitterion and neutral structures, J. Am. Chem. Soc. 122 (2000) 10159–10162.
[24] C. Schmuck, W. Wienand, Highly stable self-assembly in water: ion pair driven dimerization of a guanidiniocarbonyl pyrrole carboxylate zwitterion, J. Am. Chem. Soc. 125 (2003) 452–459.
[25] R. Simkovitch, N. Karton-Lifshin, S. Shomer, D. Shabat, D. Huppert, Ultrafast excited-state proton transfer to the solvent occurs on a hundred-femtosecond time-scale, J. Phys. Chem. A 117 (2013) 3405–3413.
[26] K. Choi, A.D. Hamilton, A dual channel fluorescence chemosensor for anions involving intermolecular excited state proton transfer, Angew. Chem. Int. Ed. 40 (2001) 3912–3915.
[27] F. Yu, P. Li, G. Li, G. Zhao, T. Chu, K. Han, A near-IR reversible fluorescent probe modulated by selenium for monitoring peroxynitrite and imaging in living cells, J. Am. Chem. Soc. 133 (2011) 11030–11033.
[28] E. Runge, E.K.U. Gross, Density-functional theory for time-dependent systems, Phys. Rev. Lett. 52 (1984) 997–1000.
[29] M.W. Schmidt, K.K. Baldridge, J.A. Boatz, S.T. Elbert, M.S. Gordon, J.H. Jensen, S. Koseki, N. Matsunaga, K.A. Nguyen, S.J. Su, T.L. Windus, M. Dupuis, J.A. Montgomery, General atomic and molecular electronic-structure system, J. Comput. Chem. 14 (1993) 1347–1363.
[30] F.L. Hirshfeld, Bonded-atom fragments for describing molecular charge densities, Theor. Chim. Acta 44 (1977) 129–138.
[31] R. Bader, T.T. Nguyen-Dang, Y. Tal, A topological theory of molecular structure, Rep. Prog. Phys. 44 (1981) 893.
[32] S. Grimme, J. Antony, S. Ehrlich, H. Krieg, A consistent and accurate ab initio parametrization of density functional dispersion correction (DFT-D) for the 94 elements H-Pu, J. Chem. Phys. 132 (2010), 154104. .
[33] M.J. Frisch, G.W. Trucks, H.B. Schlegel, G.E. Scuseria, M.A. Robb, J.R. Cheeseman, G. Scalmani, V. Barone, G.A. Petersson, H. Nakatsuji, X. Li, M. Caricato, A.V. Marenich, J. Bloino, B.G. Janesko, R. Gomperts, B. Mennucci, H.P. Hratchian, J.V. Ortiz, A.F. Izmaylov, J.L. Sonnenberg, Williams, F. Ding, F. Lipparini, F. Egidi, J. Goings, B. Peng, A. Petrone, T. Henderson, D. Ranasinghe, V.G. Zakrzewski, J. Gao, N. Rega, G. Zheng, W. Liang, M. Hada, M. Ehara, K. Toyota, R. Fukuda, J. Hasegawa, M. Ishida, T. Nakajima, Y. Honda, O. Kitao, H. Nakai, T. Vreven, K. Throssell, J.A. Montgomery Jr., J.E. Peralta, F. Ogliaro, M.J. Bearpark, J.J. Heyd, E.N. Brothers, K.N. Kudin, V.N. Staroverov, T.A. Keith, R. Kobayashi, J. Normand, K. Raghavachari, A.P. Rendell, J.C. Burant, S.S. Iyengar, J. Tomasi, M. Cossi, J.M. Millam, M. Klene, C. Adamo, R. Cammi, J.W. Ochterski, R.L. Martin, K. Morokuma, O. Farkas, J.B. Foresman, D.J. Fox, Gaussian 16, Wallingford, CT, 2016.
[34] T. Lu, F. Chen, Multiwfn: a multifunctional wavefunction analyzer, J. Comput. Chem. 33 (2012) 580–592.
[35] Y. Zhao, D.G. Truhlar, The M06 suite of density functionals for main group thermochemistry, thermochemical kinetics, noncovalent interactions, excited states, and transition elements: two new functionals and systematic testing of four M06-class functionals and 12 other functionals, Theor. Chem. Accounts 120 (2008) 215–241.
[36] W.J. Hehre, Ab Initio Molecular Orbital Theory, Wiley-Interscience, 1986.
[37] F. Weigend, R. Ahlrichs, Balanced basis sets of split valence, triple zeta valence and quadruple zeta valence quality for H to Rn: design and assessment of accuracy, Phys. Chem. Chem. Phys. 7 (2005) 3297–3305.
[38] C. Adamo, V. Barone, Toward reliable density functional methods without adjustable parameters: the PBE0 model, J. Chem. Phys. 110 (1999) 6158–6170.
[39] J. Zheng, X. Xu, D.G. Truhlar, Minimally augmented Karlsruhe basis sets, Theor. Chem. Accounts 128 (2011) 295–305.
[40] A.V. Marenich, C.J. Cramer, D.G. Truhlar, Universal solvation model based on solute electron density and on a continuum model of the solvent defined by the bulk dielectric constant and atomic surface tensions, J. Phys. Chem. B 113 (2009) 6378–6396.
[41] A. Rios, T.L. Amyes, J.P. Richard, Formation and stability of organic zwitterions in aqueous solution: enolates of the amino acid glycine and its derivatives, J. Am. Chem. Soc. 122 (2000) 9373–9385.
[42] P. Politzer, J.S. Murray, The fundamental nature and role of the electrostatic potential in atoms and molecules, Theor. Chem. Accounts 108 (2002) 134–142.
[43] P. Stephens, F. Devlin, C. Chabalowski, M.J. Frisch, Ab initio calculation of vibrational absorption and circular dichroism spectra using density functional force fields, J. Phys. Chem. 98 (1994) 11623–11627.
[44] T. Yanai, D.P. Tew, N.C. Handy, A new hybrid exchange–correlation functional using the coulomb-attenuating method (CAM-B3LYP), Chem. Phys. Lett. 393 (2004) 51–57.
[45] J.D. Chai, M. Head-Gordon, Long-range corrected hybrid density functionals with damped atom–atom dispersion corrections, Phys. Chem. Chem. Phys. 10 (2008) 6615–6620.
[46] G.H. Fan, K.L. Han, G.Z. He, Time-dependent density functional-based tight-bind method efficiently implemented with OpenMP parallel and GPU acceleration, Chin. J. Chem. Phys. 26 (2013) 635–645.
[47] Y. Tawada, T. Tsuneda, S. Yanagisawa, T. Yanai, K. Hirao, A long-range-corrected time-dependent density functional theory, J. Chem. Phys. 120 (2004) 8425–8433.